

## EDGE ARTICLE

View Article Online  
View Journal | View Issue

## Structural and mechanistic investigation of a cationic hydrogen-substituted ruthenium silylene catalyst for alkene hydrosilation†

Cite this: *Chem. Sci.*, 2013, **4**, 3882

Meg E. Fasulo, Mark C. Lipke and T. Don Tilley\*

The cationic ruthenium silylene complex  $[\text{Cp}^*(\text{iPr}_3\text{P})\text{Ru}(\text{H})_2(\text{SiHMe}_3)][\text{CB}_{11}\text{H}_6\text{Br}_6]$ , a catalyst for olefin hydrosilations with primary silanes, was isolated and characterized by X-ray crystallography. Relatively strong interactions between the silylene Si atom and Ru–H hydride ligands appear to reflect a highly electrophilic silicon center. The mechanism of olefin hydrosilation was examined by kinetics measurements and other experiments to provide the first experimentally determined mechanism for the catalytic cycle. This mechanism involves a fast, initial addition of the Si–H bond of the silylene complex to the olefin. Subsequent elimination of the product silane produces an unsaturated intermediate, which can be reversibly trapped by olefin or intercepted by the silane substrate. The latter reaction pathway involves activation of the reactant silane by Si–H oxidative addition and  $\alpha$ -hydrogen migration to regenerate the key silylene intermediate.

Received 5th June 2013  
Accepted 29th July 2013

DOI: 10.1039/c3sc51585k

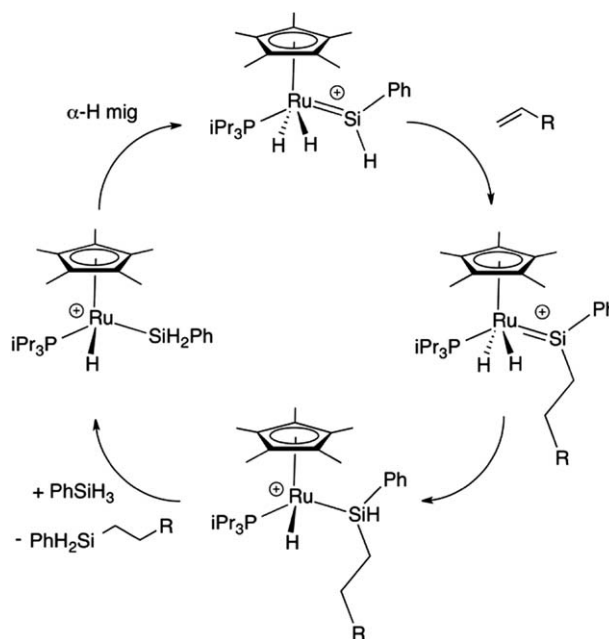
www.rsc.org/chemicalscience

## Introduction

Hydrosilation, the addition of an Si–H bond across an unsaturated bond ( $\text{C}=\text{C}$ ,  $\text{C}=\text{O}$ ,  $\text{C}=\text{N}$ , *etc.*), is an extremely important chemical transformation in the laboratory and in large-scale industrial applications.<sup>1</sup> Commercial hydrosilations utilize expensive platinum-based catalysts, which are highly effective but somewhat limited with respect to selectivities and substrate scope.<sup>2</sup> The performance of these catalysts is generally understood within the context of the Chalk–Harrod or modified Chalk–Harrod mechanisms, which account for the observed activity as well as the side reactions which lower selectivity.<sup>3</sup> Because of the limitations associated with this catalysis, and especially due to the rising cost of platinum, there is considerable interest in the discovery of new types of hydrosilation catalysts. In this context, the discovery of active hydrosilation catalysts based on more cost-effective transition metals is an important research objective.<sup>4</sup> Progress toward this goal should be greatly facilitated by identification of new mechanisms for catalytic hydrosilation.

Several recent investigations point to the potential utility of transition metal silylene complexes as reactive intermediates in the catalytic hydrosilation of olefins.<sup>5–9</sup> The initial discovery of hydrosilation catalyzed by a silylene complex,  $[\text{Cp}^*(\text{iPr}_3\text{P})\text{RuH}_2(\text{SiHPh} \cdot \text{Et}_2\text{O})][\text{B}(\text{C}_6\text{F}_5)_4]$  (**1**), implicated a new hydrosilation mechanism involving direct addition of the silylene Si–H bond to an olefin (Scheme 1).<sup>6</sup> The silylene ligand appears to be regenerated in the catalytic cycle by oxidative addition of an Si–H bond, followed by 1,2-migration of a second hydrogen from silicon to ruthenium. Additionally, the silylene functionality is necessary for catalysis, since the related silyl complexes

$\text{RuH}_2(\text{SiHPh} \cdot \text{Et}_2\text{O})][\text{B}(\text{C}_6\text{F}_5)_4]$  (**1**), implicated a new hydrosilation mechanism involving direct addition of the silylene Si–H bond to an olefin (Scheme 1).<sup>6</sup> The silylene ligand appears to be regenerated in the catalytic cycle by oxidative addition of an Si–H bond, followed by 1,2-migration of a second hydrogen from silicon to ruthenium. Additionally, the silylene functionality is necessary for catalysis, since the related silyl complexes



Scheme 1

Department of Chemistry, University of California–Berkeley, Berkeley, CA, 94720, USA.  
E-mail: [tdtilley@berkeley.edu](mailto:tdtilley@berkeley.edu)

† Electronic supplementary information (ESI) available: Synthetic details, characterization data, crystallographic data, and computational details. CCDC 942935. For ESI and crystallographic data in CIF or other electronic format see DOI: 10.1039/c3sc51585k

$\text{Cp}^*(\text{Pr}_3\text{P})\text{RuH}_2(\text{SiHPhOTf})$  and  $\text{Cp}^*(\text{Pr}_3\text{P})\text{Ru}(\text{H})\text{Cl}(\text{SiH}_2\text{Ph})$  are not active catalysts. This catalysis features a strict selectivity for primary silanes (to exclusively give secondary silane products), and no reactivity is observed with secondary and tertiary silanes. Additionally, these olefin hydrosilations are highly selective in exclusively producing anti-Markovnikov products. Typical byproducts of hydrosilation catalysis with platinum, such as vinyl silanes, isomerized olefin, and silane redistribution products, are not observed with **1** as catalyst. Studies with analogous osmium silylene complexes indicate that the cationic nature of the catalytic species is required for insertion of the olefin into the Si–H bond.<sup>7</sup>

Given the potential utility of new catalysis based on reactions of a silylene ligand, it is important to obtain detailed mechanistic information for hydrosilations catalyzed by **1** and related complexes. Current understanding of the mechanism is based only on studies of stoichiometric transformations, and by DFT investigations on simplified model systems.<sup>8</sup> Significantly, kinetic studies of the catalytic process have not been reported, and structural information on key catalytic species of the type  $[\text{Cp}^*(\text{Pr}_3\text{P})\text{RuH}_2(=\text{SiHR})]^+$  has not been available. In addition, kinetic studies on catalysis by **1** has been complicated by lack of a suitable solvent that is unreactive and nonvolatile over an appropriate temperature range. Here, we report the synthesis and structural characterization of  $[\text{Cp}^*(\text{Pr}_3\text{P})\text{RuH}_2(=\text{SiHMe})][\text{CB}_{11}\text{H}_6\text{Br}_6]$  (**2**), a hydrosilation catalyst and model for the key silylene intermediate. Most significantly, kinetic studies with this catalyst provide the first detailed description of the mechanism of this silylene-mediated hydrosilation, and provide a firm basis for future catalyst development.

## Results and discussion

### Synthesis and structural characterization of cationic silylene complex $[\text{Cp}^*(\text{Pr}_3\text{P})\text{RuH}_2(=\text{SiHMe})]^+$ (**2**)

A primary objective of this investigation was to obtain detailed structural data for a  $[\text{Cp}^*(\text{Pr}_3\text{P})\text{RuH}_2(=\text{SiHR})]^+$  silylene complex, since such species are thought to engage in the key Si–C bond-forming event in hydrosilation catalysis. Interestingly, DFT calculations on the simplified model systems  $[\text{Cp}(\text{H}_3\text{P})\text{RuH}_2(=\text{SiHR})]^+$  ( $\text{R}=\text{H}$ ,<sup>8a</sup>  $\text{Ph}^{8b}$ ) predict a distorted four-legged piano stool structure, with the presence of two strong ruthenium hydride–silicon interactions. Numerous initial efforts to obtain X-ray quality crystals for structural studies focused on cationic silylene complexes containing the  $[\text{B}(\text{C}_6\text{F}_5)_4]^-$  anion, and were not successful. Thus, attention turned to use of other weakly coordinating anions, and in this regard the carborane anion  $[\text{CB}_{11}\text{H}_6\text{Br}_6]^-$  seemed particularly promising given its proven utility in providing crystalline samples of iridium silylene complexes and other cationic silicon species.<sup>10</sup>

Reaction of  $\text{Cp}^*(\text{Pr}_3\text{P})\text{RuH}_2(\text{SiHMeOTf})$ <sup>11</sup> with  $[\text{Et}_3\text{Si}][\text{CB}_{11}\text{H}_6\text{Br}_6]$ <sup>12</sup> in  $\text{C}_6\text{H}_5\text{F}$  followed by precipitation with pentane provided  $[\text{Cp}^*(\text{Pr}_3\text{P})\text{RuH}_2(=\text{SiHMe})][\text{CB}_{11}\text{H}_6\text{Br}_6]$  (**2**) as an orange solid. The <sup>29</sup>Si NMR spectrum reveals a resonance at 228.7 ppm, and in the <sup>1</sup>H NMR spectrum the ruthenium hydride ligands at –11.35 ppm display a <sup>2</sup>J<sub>SiH</sub> coupling constant of 62.3 Hz. These values are similar to those observed for the

analogous complex  $[\text{Cp}^*(\text{Pr}_3\text{P})\text{RuH}_2(=\text{SiHMe})][\text{B}(\text{C}_6\text{F}_5)_4]$  (<sup>29</sup>Si = 228.9 ppm, <sup>2</sup>J<sub>SiH</sub> = 58.2 Hz).<sup>11</sup> Interestingly, the borate and carborane salts display different thermal stabilities – while  $[\text{Cp}^*(\text{Pr}_3\text{P})\text{RuH}_2(=\text{SiHMe})][\text{B}(\text{C}_6\text{F}_5)_4]$  can be stored for 1 to 2 weeks at –35 °C before significant decomposition, **2** can be stored for 2 months at –35 °C without decomposition and is stable in  $\text{C}_6\text{D}_5\text{Br}$  solution at room temperature for *ca.* one week.

Single crystals suitable for X-ray diffraction were grown by vapor diffusion of pentane into a solution of **2** in  $\text{C}_6\text{H}_5\text{F}$  over 48 h at –35 °C (Fig. 1). No interactions are observed between the carborane anion and the silicon center. The Ru–Si bond distance of 2.246(1) Å is slightly longer than analogous distances in the neutral ruthenium silylene complexes  $\text{Cp}^*(\text{CO})(\text{H})\text{Ru}=\text{SiH}[\text{C}(\text{SiMe}_3)_3]$  (2.220(2) Å)<sup>13</sup> and  $\text{Cp}^*(\text{Pr}_2\text{MeP})(\text{H})\text{Ru}=\text{SiH}(\text{Trip})$  (2.205(1) Å)<sup>14</sup> but is similar to that found in the cationic complex  $[\text{Cp}^*(\text{Me}_3\text{P})_2\text{Ru}=\text{SiMe}_2][\text{B}(\text{C}_6\text{F}_5)_4]$  (2.238(3) Å).<sup>15</sup> This observed bond lengthening may be attributed to a greater contribution from a silicenium resonance form, with a concomitant reduction in the Ru–Si bond order.<sup>7</sup> The ruthenium hydride ligands were located in the Fourier difference map; however, the position of H(2) was not stable under refinement and was fixed. The Ru–H(1) distance of 1.73(6) Å is longer than analogous Ru–H distances observed in  $\text{Cp}^*(\text{Pr}_3\text{P})\text{Ru}(\text{H})_2(\text{SiHMeCl})$ <sup>16</sup> (Ru–H(1) = 1.50(9) Å; Ru–H(2) = 1.59(7) Å) and  $\text{Cp}^*(\text{Pr}_3\text{P})\text{Ru}(\text{H})_2(\text{SiPh}_2\text{OTf})$ <sup>11</sup> (Ru–H(1) = 1.41(4) Å; Ru–H(2) = 1.51(5) Å), and the Si···H(1) distance of 1.74(6) Å is remarkably short, indicating a strong Ru–H···Si interaction in **2**. For comparison, the neutral complex  $\text{Cp}^*(\text{Pr}_2\text{MeP})(\text{H})\text{Ru}=\text{SiH}(\text{Trip})$  displays a RuH···Si distance of 2.21(4) Å.<sup>14</sup> The silicon atom is coplanar with P, Ru, and the Cp\* centroid (sum of angles = 360.0(5)°) suggesting that the hydrides may be equivalent and related by a molecular mirror plane.

The strong distortion of **2** away from an idealized four-legged piano stool structure, with the hydride ligands significantly displaced toward silicon, is reminiscent of similar distortions found in piano-stool silyl hydride complexes of ruthenium and is usually attributed to donation of hydride electron density to the electrophilic silicon center.<sup>17</sup> For  $\text{Cp}^*(\text{Pr}_3\text{P})\text{Ru}(\text{H})_2(\text{SiHMeCl})$ ,

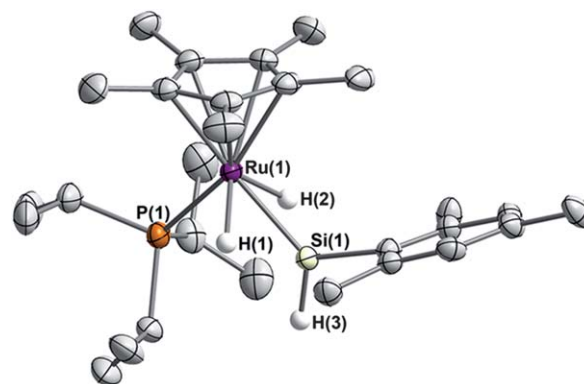


**Fig. 1** Molecular structure of **2** displaying thermal ellipsoids at the 50% probability level. Selected H-atoms, carborane anion, and fluorobenzene molecule have been omitted for clarity. Selected bond lengths (Å): Ru(1)–Si(1) = 2.2461(13), Ru(1)–P(1) = 2.3662(12), Ru(1)–H(1) = 1.73(6), Ru(1)–H(2) = 1.5981(4), Si(1)–H(3) = 1.32(6).

this distortion from a regular, piano-stool geometry results in P–Ru–H angles (78, 79°) that are substantially wider than the Si–Ru–H angles (60, 64°). The stronger distortion for **2**, reflected in a greater difference between the P–Ru–H (80, 85°) and Si–Ru–H (50, 54°) angles, appears to result from the more strongly electrophilic nature of the three-coordinate, sp<sup>2</sup>-hybridized silicon center in this type of cationic structure.<sup>18</sup> In addition, the small hydrogen substituent at the silicon center of **2** allows the complex to readily adopt a conformation that maximizes interactions of the hydrides with the formally empty p orbital at silicon, with the silylene plane bisecting the H–Ru–H angle.<sup>19</sup> Thus, the silicon–hydride interactions appear to be a consequence of the unusually electrophilic nature of the silicon center and **2**, and in catalysis must be readily displaced by nucleophilic attack of an incoming olefin substrate.

The structure and bonding in **2** were examined by DFT calculations to provide additional information on the nature of the Ru–H–Si interactions. The solid-state structure of **2** was used as a starting point for a DFT geometry optimization calculation that indicated the presence of two equivalent, strong Si–H interactions (Si–H distances 1.683, 1.676 Å for **2-DFT**).<sup>20</sup> These Si–H distances are quite short, and suggest that **2** could be described as having a structure featuring an η<sup>3</sup>-H<sub>2</sub>SiHMe ligand.<sup>18</sup> This bonding description is supported by NBO and NMLO calculations on **2-DFT**, which are consistent with the presence of two Si–H bonds that donate strongly to the ruthenium center. Additionally, these calculations do not indicate the presence of a strong, direct σ bond between the ruthenium and silicon. Thus, **2** appears to feature considerable η<sup>3</sup>-H<sub>2</sub>SiHMe character and is therefore related to [PhBP<sub>3</sub>]RuH(η<sup>3</sup>-H<sub>2</sub>SiRR') complexes that also exhibit substantial electrophilicity at silicon.<sup>18</sup> However, the NMR data for **2** (<sup>29</sup>Si δ 228.7 ppm, J<sub>SiH</sub> = 62.3 Hz) indicate that this complex features a higher degree of silylene character and weaker Si–H interactions (for [PhBP<sub>3</sub>]RuH(η<sup>3</sup>-H<sub>2</sub>SiRR'); <sup>29</sup>Si δ ≈ 150 ppm, J<sub>SiH</sub> ≈ 100 Hz). These comparisons suggest that there is a strong relationship between ruthenium(IV) silylene dihydride and ruthenium(II) η<sup>3</sup>-silane structures, and perhaps a continuum represented by the contributing resonance structures of Scheme 2. Complete cleavage of two Si–H bonds in the coordinated silane results in the dihydride structure on the left, whereas incomplete Si–H activation leads to the η<sup>3</sup>-silane complex on the right. This is consistent with observed similarities between silylene dihydride and η<sup>3</sup>-silane complexes,<sup>18</sup> and is related to the continuum that has been established for η<sup>2</sup>-HSiR<sub>3</sub> and silyl hydride complexes.<sup>21</sup>

### Catalytic hydrosilation with **2**

Compound **2** was evaluated as a catalyst for the hydrosilation of a variety of olefins, with the primary silanes PhSiH<sub>3</sub> and CySiH<sub>3</sub> (Table 1). In a typical hydrosilation experiment, equimolar amounts of the primary silane and the olefin were added to a

C<sub>6</sub>D<sub>5</sub>Br solution containing 1 mol% loading of **2** and an internal standard. The reaction temperature was then raised to 80 °C, and reactions were allowed to proceed for 1 h. As observed for both [Cp\*(<sup>1</sup>Pr<sub>3</sub>P)RuH<sub>2</sub>(SiHPh·Et<sub>2</sub>O)][B(C<sub>6</sub>F<sub>5</sub>)<sub>4</sub>]<sup>6</sup> and [(PNP)(H)Ir=Si(H)Me][B(C<sub>6</sub>F<sub>5</sub>)<sub>4</sub>],<sup>22</sup> the catalysis is regioselective and exclusively produces the anti-Markovnikov, secondary silane product (H<sub>2</sub>SiRR'), which is inactive to further hydrosilation.

Unlike **1**, compound **2** catalyzes the redistribution of PhSiH<sub>3</sub> under these reaction conditions, and this results in lower yields for the main hydrosilation product. For example, the catalytic reaction mixture of PhSiH<sub>3</sub> and 1-hexene after 1 h at 80 °C in C<sub>6</sub>D<sub>5</sub>Br contains PhHexSiH<sub>2</sub> (60%), PhSiH<sub>3</sub> (8%), HexSiH<sub>3</sub> (19%), and Ph<sub>2</sub>SiH<sub>2</sub> (10%). For comparison, the B(C<sub>6</sub>F<sub>5</sub>)<sub>4</sub><sup>−</sup> analogue of **2**, [Cp\*(<sup>1</sup>Pr<sub>3</sub>P)RuH<sub>2</sub>(=SiHMe)][B(C<sub>6</sub>F<sub>5</sub>)<sub>4</sub>],<sup>11</sup> produces only the hydrosilation product PhHexSiH<sub>2</sub> (98%) under the same reaction conditions. The redistribution chemistry associated with **2** was found to be dependent on the nature of the organosilane substrate, as the alkylsilane substrate CySiH<sub>3</sub> results in no redistribution products under the same conditions with **2** as catalyst. In the absence of olefin, **2** reacted with 10 equiv. of PhSiH<sub>3</sub> at 80 °C in C<sub>6</sub>D<sub>5</sub>Br over 1 h to give Ph<sub>3</sub>SiH (16%), Ph<sub>2</sub>SiH<sub>2</sub> (27%), PhSiH<sub>3</sub> (27%), and SiH<sub>4</sub> (30%). Under analogous conditions, no redistribution is observed for [Cp\*(<sup>1</sup>Pr<sub>3</sub>P)RuH<sub>2</sub>(=SiHMe)][B(C<sub>6</sub>F<sub>5</sub>)<sub>4</sub>] with 10 equiv. of PhSiH<sub>3</sub>. These interesting results imply that the anion plays a crucial role in defining the catalytic chemistry. A detailed explanation for this difference is currently lacking, but it would seem to reflect the nature of cation–anion interactions in solution. In this context, note that redistribution at silicon has been shown to occur *via* bimolecular reactions of neutral silyl and cationic silylene Cp\*Ru complexes in solution.<sup>23</sup> Interestingly, a ten-fold decrease in the concentration of **2** gave much lower conversion of 10 equiv. of PhSiH<sub>3</sub> at 80 °C in C<sub>6</sub>D<sub>5</sub>Br over 1 h to the redistribution products Ph<sub>2</sub>SiH<sub>2</sub> (5%) and SiH<sub>4</sub> (3%) (92% of the PhSiH<sub>3</sub> remained).

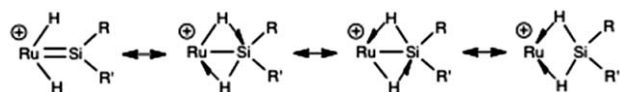
### Mechanistic studies on hydrosilation with **2**

Mechanistic studies were undertaken using CySiH<sub>3</sub> and 1-octene as substrates, to avoid possible complications from silane redistribution. Kinetic measurements were monitored by loss of silane at 80 °C in bromobenzene-*d*<sub>5</sub>, and the appearance

Table 1 Catalytic hydrosilation by **2**<sup>a</sup>

Silane	Alkene	Yield
PhSiH <sub>3</sub>	1-Octene	73%
	1-Hexene	60%
	Cyclopentene	67%
	Cyclohexene	79%
	<i>t</i> -Butylethylene	79%
CySiH <sub>3</sub>	1-Octene	>98%
	1-Hexene	97%
	Cyclopentene	>98%
	Cyclohexene	94%
	<i>t</i> -Butylethylene	>98%

<sup>a</sup> Reactions were conducted with 1 mol% of **2** in 0.5 mL of C<sub>6</sub>D<sub>5</sub>Br at 80 °C for 1 h. Yields were determined by integration of <sup>1</sup>H NMR resonances with respect to an internal standard (C<sub>6</sub>Me<sub>6</sub>).



Scheme 2

of product correlates with silane loss. First-order dependence of the reaction rate on the concentration of **2** was established by varying the loading of catalyst **2** from 1 to 4 mol% (Fig. S1†). Preliminary studies indicated that the reaction is not first order in olefin and suggested an inverse dependence. To determine the reaction order in olefin more precisely, pseudo-first order reaction conditions were established for various concentrations of olefin (3.2–7.5 M) with 0.16 M silane and 1 mol% catalyst **2**. For these conditions, plots of [olefin] vs.  $1/k_{\text{obs}}$  were linear, indicating an inverse-order dependence on olefin (Fig. S2†). Interestingly, the concentration of olefin influences the order of the reaction with respect to  $\text{CySiH}_3$ . At low concentrations of olefin (0.16 M), the reaction rate is independent of the concentration of  $\text{CySiH}_3$ , and depends only on the concentration of **2**. At higher concentrations of olefin (3.2–7.5 M), the reaction order in silane was determined to be first order based on linear plots of  $\ln[\text{silane}]$  vs. time (Fig. S7†), measured over 4 half-lives. This information suggests that under typical catalytic conditions (1 : 1 ratio of silane : olefin), the rate determining step does not involve silane or olefin, but that at much higher concentrations of olefin, the silane must effectively compete with the olefin for binding to the catalyst. The complex influence of olefin concentration on the reaction rate provides unanticipated, new information about the mechanism of this hydrosilation.

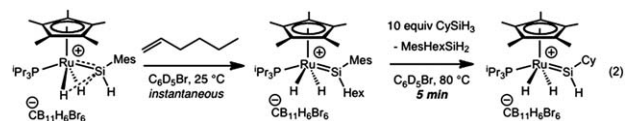
Further investigation of the catalytic mechanism involved a series of isotopic labeling experiments. An experiment to determine the kinetic isotope effect (KIE) for catalysis involved the competition reaction of 1 equiv. of 1-octene with 10 equiv. of  $\text{CySiH}_3$  and 10 equiv. of  $\text{CySiD}_3$ , in the presence of 1 mol% of **2** in  $\text{C}_6\text{D}_5\text{Br}$  at 80 °C over 1 h. The KIE was found to be  $k_{\text{H}}/k_{\text{D}} = 1.5(1)$ , which suggests that an Si–H bond is broken or formed during the rate determining step (RDS). Based on the previously suggested mechanism, there are three steps that involve cleavage of an Si–H bond: initial Si–H activation of the silane at the metal center,  $\alpha$ -H migration from silicon to ruthenium to produce the silylene ligand, and insertion of an olefin into the H-substituted silylene ligand. The elimination of the product silane involves the formation of two Si–H bonds by processes that are the reverse of the Si–H activation steps.

For the olefin insertion step, the related complex  $[\text{Cp}^*(\text{Pr}_3\text{P})\text{OsH}_2(=\text{SiH}(\text{Trip}))][\text{B}(\text{C}_6\text{F}_5)_4]^-$  was reported to exhibit an inverse KIE of  $k_{\text{H}}/k_{\text{D}} = 0.8(1)$ , and this was attributed to a secondary effect resulting from rehybridization of the silylene ligand ( $\text{Si}_{\text{sp}^2}\text{--H/D} \rightarrow \text{Si}_{\text{sp}^3}\text{--H/D}$ ) upon coordination of the olefin to silicon. To determine the KIE associated with the ruthenium system described here, a competition experiment between **2** and  $[\text{Cp}^*(\text{Pr}_3\text{P})\text{RuD}_2(=\text{SiDMes})][\text{CB}_{11}\text{H}_6\text{Br}_6]^-$  (**2-d<sub>3</sub>**) was conducted by combining 1 equiv. of **2** with 1 equiv. of **2-d<sub>3</sub>** in  $\text{C}_6\text{D}_5\text{Br}$ , followed by 0.5 equiv. of 1-octene and the internal standard  $\text{Ph}_2\text{Si}(\text{CH}_3)(\text{CD}_3)$ . After 5 min at room temperature, the distribution of products reflected an inverse KIE of  $k_{\text{H}}/k_{\text{D}} = 0.77(4)$  (by NMR spectroscopy), which may result from the secondary, rehybridization effect mentioned above. However, note that this insertion step results in a loss of the intramolecular Ru–H–Si interactions, as indicated by the lack of an observable  $^2J_{\text{SiH}}$  coupling constant in the new silylene complex (*vide infra*). This

type of structural change has previously been observed and attributed to steric influence on rotation about the metal–silicon bond, and consequently the magnitude of the non-classical Ru–H–Si interactions. Thus, the displacement of such interactions in **2** could contribute to the observed inverse KIE since the transfer of deuteride from a bridging position to a terminal position is more favorable than for hydride.<sup>24</sup> The observed difference between the KIE for the overall reaction and that for olefin insertion indicates that the latter is not the RDS. Additionally, the catalytic reaction of 1-octene and  $\text{CySiD}_3$  by **2** in  $\text{C}_6\text{D}_5\text{Br}$  resulted in a single isotopomer by  $^1\text{H}$  and  $^2\text{H}$  NMR spectroscopy, consistent with a concerted reaction (eqn (1)). The competition experiment of 10 equiv. of  $\text{CySiH}_3$ , 10 equiv. of  $\text{CySiD}_3$ , 100 equiv. of 1-octene, and 1 equiv. of **2** in  $\text{C}_6\text{D}_5\text{Br}$  at 80 °C for 1 h gave a mixture of isotopomers, preventing the determination of a KIE.



Qualitative observations provide further evidence that the RDS occurs during the exchange of the secondary silane product for the primary silane substrate to regenerate the H-substituted silylene complex. The stoichiometric reaction of **2** with 1 equiv. of 1-hexene in  $\text{C}_6\text{D}_5\text{Br}$  at room temperature proceeds instantaneously with a color change from bright orange to bright yellow to give the secondary silylene complex  $[\text{Cp}^*(\text{Pr}_3\text{P})\text{RuH}_2(=\text{SiMe}(\text{Hex}))][\text{CB}_{11}\text{H}_6\text{Br}_6]^-$  (**3**) (eqn (2)). The  $^{29}\text{Si}$  NMR spectrum reveals a resonance at 264.7 ppm, and in the  $^1\text{H}$  NMR spectrum the ruthenium hydride ligands at  $-11.62$  ppm do not display a  $^2J_{\text{SiH}}$  coupling constant, indicating little or no Ru–H $\cdots$ Si interaction.<sup>11</sup> Addition of 10 equiv. of  $\text{CySiH}_3$  to **3** in  $\text{C}_6\text{D}_5\text{Br}$  resulted in no observable reaction after 3 h at room temperature. However, heating this reaction mixture at 80 °C for 5 min resulted in complete conversion to  $[\text{Cp}^*(\text{Pr}_3\text{P})\text{RuH}_2(=\text{SiH}(\text{Cy}))][\text{CB}_{11}\text{H}_6\text{Br}_6]^-$  (eqn (2)). Efforts to observe an intermediate in the reaction of **3** with 1–10 equiv. of  $\text{CySiH}_3$  by NMR spectroscopy were unsuccessful. In order to probe the reversibility of product release, a model reaction involving 20 equiv. of  $\text{MesHexSiH}_2$  and the silylene complex  $[\text{Cp}^*(\text{Pr}_3\text{P})\text{RuH}_2(=\text{SiHMe})][\text{CB}_{11}\text{H}_6\text{Br}_6]^-$  (**2**) in  $\text{C}_6\text{D}_5\text{Br}$  solution was monitored by NMR spectroscopy. After 1 h at room temperature, an equilibrium mixture of **2** and **3** (10 : 1) was established and 0.1 equiv. of free  $\text{H}_3\text{SiMe}$  was observed in solution, indicating that product formation is somewhat reversible ( $K_{\text{eq}} \approx 2000$ ).



Activation parameters for the catalytic reaction were determined by kinetic measurements over the temperature range of 60–90 °C. An Eyring plot provides the values  $\Delta H^\ddagger = 32(2)$  kcal mol $^{-1}$ ,  $\Delta S^\ddagger = 19(1)$  J K $^{-1}$  mol $^{-1}$ , and  $\Delta G^\ddagger = 25(2)$  kcal mol $^{-1}$  (at 80 °C; Fig. S3†). If the silane exchange process ( $\text{CySiH}_3$  activation and  $\text{CyRSiH}_2$  elimination) were to have appreciable



associative character, then a negative entropy of activation might be expected. Thus, the large, positive value for  $\Delta S^\ddagger$  suggests that the rate-determining step involves dissociation of the product silane ( $\text{CyRSiH}_2$ ) from the ruthenium center prior to binding of either substrate molecule. This is consistent with the experimentally determined rate law under relatively low substrate loadings, which shows that the rate depends only on the concentration of the catalyst. Notably, this aspect of the mechanism differs from calculations of Beddie and Hall, on reaction of the model system  $[\text{Cp}(\text{H}_3\text{P})\text{RuH}_2(=\text{SiH}_2\text{Et})]^+$  with  $\text{SiH}_4$ .<sup>8a</sup> The latter study concluded that the transition state for this step involves elimination of  $\text{EtSiH}_3$  from the model complex  $[\text{Cp}(\text{H}_3\text{P})\text{RuH}(\text{SiH}_3)(\eta^2\text{-HSiH}_2\text{Et})]^+$ , which already features a new substrate molecule added to ruthenium.

From the kinetic and mechanistic information described above, the catalytic cycle of Scheme 3 is proposed. The first step involves a rapid, concerted addition of the Si–H bond of the H-substituted silylene complex **A** across the carbon–carbon double bond of the olefin substrate. This step appears to be strongly promoted by silicenium character in **A** (see resonance structures **A** and **A'** in Scheme 3),<sup>7</sup> and produces a disubstituted silylene complex (**B**) with displacement of the intramolecular Ru–H $\cdots$ Si interactions. The lack of Ru–H $\cdots$ Si interactions in **B** (indicated by the NMR data) is thought to result from the steric influence of two non-hydrogen substituents at silicon, which induces rotation about the Ru–Si bond such that donation of electron density from the lateral Ru–H bonds into a 3p orbital of the silicon center is less favorable.<sup>11,19</sup> Next, complex **B** undergoes reversible  $\alpha$ -hydride migration from ruthenium to silicon to produce the unsaturated (16 electron) ruthenium silyl complex **C**. Reductive elimination of the product Si–H bond generates an unsaturated (formally 14 e<sup>−</sup>) complex **D**, to which  $\text{CySiH}_3$  rapidly adds by oxidative addition and 1,2-hydride migration to regenerate the silylene complex **A**. Complex **D**, which is implicated by the kinetic data, was not observed but it may exist as a

complex of  $[\text{Cp}^*(\text{Pr}_3\text{P})\text{Ru}]^+$  stabilized by coordinated solvent. The substrate/product exchange may be somewhat reversible, as indicated by the observed reaction of **2** with  $\text{MesHexSiH}_2$ , but the displacement of the secondary silane product by the primary silane appears to be strongly favored.

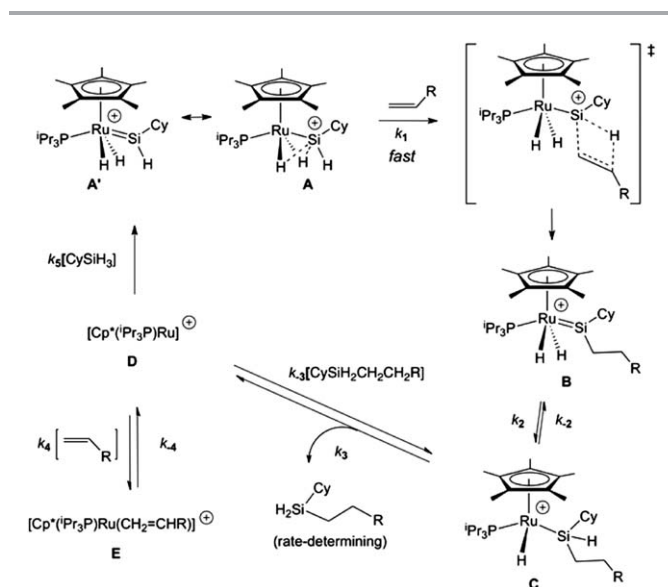
Notably, under high concentrations of olefin, **D** can instead be trapped by olefin to give **E**. The formation of **E** represents a non-productive equilibrium that is reflected in the inverse-order rate dependence on olefin. Experiments to observe a complex of type **E** involved addition of 1–20 equiv. of 1-octene to **2** in  $\text{C}_6\text{D}_5\text{Br}$ , but NMR spectra of the resulting solutions at  $-30$  to  $25^\circ\text{C}$  did not provide definitive evidence for the formation of an olefin complex, and were limited by the freezing point of the solvent ( $-30.8^\circ\text{C}$ ). For the product forming pathway,  $\text{CySiH}_3$  must compete with the olefin for binding to ruthenium, and thus the reaction is first order in  $\text{CySiH}_3$  when the concentration of olefin is high. Under these conditions, saturation behavior was observed for  $\text{CySiH}_3$ , and a maximum rate was observed at concentrations of 3.5 M silane and greater (Fig. S8†).

The rate expression for consumption of the reactant silane in the catalytic cycle in Scheme 3, derived from application of the steady state approximation to species **D**, is given in eqn (3) (see ESI†). This rate law predicts that saturation should be observed with respect to [silane] when  $k_5[\text{silane}]$  is much larger than the other terms in the denominator. However, at higher concentrations of olefin or product, the [silane] term in the numerator is not canceled by this same term in the denominator, and the reaction becomes first order with respect to [silane], and inverse order in [olefin] or [product]. Thus, this rate law is consistent with the aforementioned experimental observations for this system, including the variable dependence of rate on [silane] and the inverse dependence on [olefin]. Additionally, under normal catalytic conditions, a silylene complex consistent with structure **B** was observed by NMR spectroscopy as the resting state of the catalytic cycle, as expected when [olefin] is too small to influence the reaction rate (*i.e.* **E** is small). Under these conditions, the rate of consumption of [silane] decreases at high conversion (>85% conversion), which is consistent with an inverse dependence on [product] at relatively high concentrations of product (Fig. S4†).

$$\frac{d[\text{silane}]}{dt} = \frac{-k_5[\text{silane}](k_3K_2[\text{B}] + k_{-4}[\text{E}])}{(k_{-3}[\text{product}] + k_4[\text{alkene}] + k_5[\text{silane}])} \quad (3)$$

## Conclusions

In conclusion, use of the anion  $[\text{CB}_{11}\text{H}_6\text{Br}_6]^-$  has enabled a structural analysis of the cationic silylene complex  $[\text{Cp}^*(\text{Pr}_3\text{P})\text{-RuH}_2(\text{SiHMe})][\text{CB}_{11}\text{H}_6\text{Br}_6]$  (**2**), which exhibits very short Ru–H $\cdots$ Si distances. These short contacts appear to reflect the presence of a strongly electrophilic silicon center, which is a key chemical property associated with hydrosilation activity. In the catalytic cycle, nucleophilic attack of the alkene onto the silicon center directly precedes insertion of the alkene into the Si–H bond of a silylene ligand.<sup>6–8</sup> Additionally, complex **2** displays greater thermal stability relative to that of the  $[\text{B}(\text{C}_6\text{F}_5)_4]^-$  analogue **1**, allowing for in-depth kinetic and mechanistic studies. Most



Scheme 3

importantly, these investigations provide the first experimental basis for a detailed mechanism of the catalytic cycle associated with silylene-mediated alkene hydrosilation. Interestingly, activation of the olefin is relatively rapid in this catalysis, and the rate-determining process is associated with elimination of the product silane. These studies provide a working model for the design of less expensive, more efficient, and/or more selective catalysts that operate *via* related mechanisms.

## Notes and references

- (a) D. Troegel and J. Stohrer, *Coord. Chem. Rev.*, 2011, **255**, 1440–1459; (b) B. Marciniec, *Silicon Chem.*, 2002, **1**, 155; (c) M. A. Brook, *Silicon in Organic, Organometallic, and Polymer Chemistry*, Wiley, New York, 2000; (d) I. Ojima, Z. Li and J. Zhu, *The Chemistry of Organic Silicon Compounds*, Wiley, Avon, 1998, ch. 29.
- (a) J. L. Speier, J. A. Webster and G. H. Barnes, *J. Am. Chem. Soc.*, 1957, **79**, 974–979; (b) B. D. Karstedt, US Patent 3,775,452, 1973; (c) J. Stein, L. N. Lewis, Y. Gao and R. A. Scott, *J. Am. Chem. Soc.*, 1999, **121**, 3693–3703.
- (a) A. J. Chalk and J. F. Harrod, *J. Am. Chem. Soc.*, 1965, **87**, 16–21; (b) F. Seitz and M. S. Wrighton, *Angew. Chem., Int. Ed. Engl.*, 1988, **27**, 289–291; (c) S. B. Duckett and R. N. Perutz, *Organometallics*, 1992, **11**, 90–98.
- (a) J. Koller and R. G. Bergman, *Organometallics*, 2012, **31**, 2530–2533; (b) J. Yang and T. D. Tilley, *Angew. Chem., Int. Ed.*, 2010, **49**, 10186–10188; (c) S. C. Bart, E. Lobkovsky and P. J. Chirik, *J. Am. Chem. Soc.*, 2004, **126**, 13794–13807; (d) M. Brookhart and B. E. Grant, *J. Am. Chem. Soc.*, 1993, **115**, 2151–2156.
- R. Waterman, P. G. Hayes and T. D. Tilley, *Acc. Chem. Res.*, 2007, **40**, 712–719.
- P. B. Glaser and T. D. Tilley, *J. Am. Chem. Soc.*, 2003, **125**, 13640–13641.
- P. G. Hayes, C. Beddie, M. B. Hall, R. Waterman and T. D. Tilley, *J. Am. Chem. Soc.*, 2006, **128**, 428–429.
- (a) C. Beddie and M. B. Hall, *J. Am. Chem. Soc.*, 2004, **126**, 13564–13565; (b) U. Bohme, *J. Organomet. Chem.*, 2006, **691**, 4400–4410.
- Transition metal silylene complexes have also been proposed as intermediates in the catalytic hydrosilation of carbonyl compounds. See: (a) N. Schneider, M. Finger, C. Haferkemper, S. Bellemin-Laponnaz, P. Hofmann and L. H. Gade, *Angew. Chem., Int. Ed.*, 2009, **48**, 1609–1613; (b) P. Gigler, B. Bechlars, W. A. Herrmann and F. E. Kühn, *J. Am. Chem. Soc.*, 2011, **133**, 1589–1596.
- (a) E. Calimano and T. D. Tilley, *Organometallics*, 2010, **27**, 1680–1692; (b) C. A. Reed, *Acc. Chem. Res.*, 1998, **31**, 133–139; (c) K.-C. Kim, C. A. Reed, D. W. Elliott, L. J. Mueller, F. Tham, L. Lin and J. B. Lambert, *Science*, 2002, **297**, 825–827; (d) Z. Xie, R. Bau, A. Benesi and C. A. Reed, *Organometallics*, 1995, **14**, 3933–3941.
- M. E. Fasulo, P. B. Glaser and T. D. Tilley, *Organometallics*, 2011, **30**, 5524–5531.
- C. A. Reed, *Acc. Chem. Res.*, 2010, **43**, 121–128.
- M. Ochiai, H. Hashimoto and H. Tobita, *Angew. Chem., Int. Ed.*, 2007, **46**, 8192–8194.
- P. G. Hayes, R. Waterman, P. B. Glaser and T. D. Tilley, *Organometallics*, 2009, **28**, 5082–5089.
- S. K. Grumbine, T. D. Tilley, F. P. Arnold and A. L. Rheingold, *J. Am. Chem. Soc.*, 1994, **116**, 5495–5496.
- B. K. Campion, R. H. Heyn and T. D. Tilley, *J. Chem. Soc., Chem. Commun.*, 1992, 1201–1203.
- (a) M. A. Rankin, D. F. MacLean, G. Schatte, R. McDonald and M. Stradiotto, *J. Am. Chem. Soc.*, 2007, **129**, 15855–15864; (b) A. L. Osipov, S. M. Gerdov, L. G. Kuzmina, J. A. K. Howard and G. I. Nikonov, *Organometallics*, 2005, **24**, 587–602; (c) S. B. Duckett, L. G. Kuzmina and G. I. Nikonov, *Inorg. Chem. Commun.*, 2000, **3**, 126–128; (d) V. Rodriguez, B. Donnadiou, S. Sabo-Etienne and B. Chaudret, *Organometallics*, 1998, **17**, 3809–3814.
- M. C. Lipke and T. D. Tilley, *J. Am. Chem. Soc.*, 2011, **133**, 16374–16377.
- A. Shinohara, J. McBee and T. D. Tilley, *Inorg. Chem.*, 2009, **48**, 8081–8083.
- DFT calculations were performed with Gaussian 09 using the B3PW91 functional and LANL2DZ/6-31G\*\* basis sets for Ru/main group elements, respectively.
- (a) U. Schubert, *Adv. Organomet. Chem.*, 1990, **30**, 151–187; (b) W. Scherer, P. Meixner, J. E. Barquera-Lozada, C. Hauf, A. Obenhuber, A. Brück, D. J. Wolstenholme, K. Ruhland, D. Leusser and D. Stalke, *Angew. Chem., Int. Ed.*, 2013, **52**, 6092–6096.
- E. Calimano and T. D. Tilley, *J. Am. Chem. Soc.*, 2008, **130**, 9226–9227.
- S. R. Klei, T. D. Tilley and R. G. Bergman, *Organometallics*, 2002, **21**, 3376–3387.
- R. B. Calvert and J. R. Shapley, *J. Am. Chem. Soc.*, 1978, **100**, 7726–7727.